Food Chemistry: X 22 (2024) 101507

Contents lists available at ScienceDirect

Food Chemistry: X

journal homepage: www.sciencedirect.com/journal/food-chemistry-x

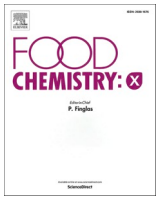

Pseudo-Siamese network combined with label-free Raman spectroscopy for the quantification of mixed trace amounts of antibiotics in human milk: A feasibility study

Jing-Yi Mou [a,b,1], Muhammad Usman [c,1], Jia-Wei Tang [a,1], Quan Yuan [a,c], Zhang-Wen Ma [d,e], Xin-Ru Wen [c], Zhao Liu [b,f,*], Liang Wang [a,g,h,i,**]

[a] Laboratory Medicine, Guangdong Provincial People's Hospital (Guangdong Academy of Medical Sciences), Southern Medical University, Guangzhou, Guangdong Province, China
[b] Department of Clinical Medicine, School of the 1st Clinical Medicine, Xuzhou Medical University, Xuzhou, Jiangsu Province, China
[c] School of Medical Informatics and Engineering, Xuzhou Medical University, Xuzhou, Jiangsu Province, China
[d] Jiangsu Key Laboratory of New Drug Research and Clinical Pharmacy, School of Pharmacy, Xuzhou Medical University, Xuzhou, Jiangsu Province, China
[e] Department of Pharmaceutical Analysis, School of Pharmacy, Xuzhou Medical University, Xuzhou, Jiangsu Province, China
[f] Department of Thyroid and Breast Surgery, Affiliated Hospital of Xuzhou Medical University, Xuzhou, Jiangsu Province, China
[g] Division of Microbiology and Immunology, School of Biomedical Sciences, The University of Western Australia, Crawley, Western Australia, Australia
[h] School of Agriculture and Food Sustainability, University of Queensland, Brisbane, Queensland, Australia
[i] Center for Precision Health, School of Medical and Health Sciences, Edith Cowan University, Perth, Western Australia, Australia

ARTICLE INFO

Keywords:
Tetracycline
Doxycycline
Human milk
Surface-enhanced Raman scattering
OPLS-DA
Machine learning algorithms

ABSTRACT

The utilization of antibiotics is prevalent among lactating mothers. Hence, the rapid determination of trace amounts of antibiotics in human milk is crucial for ensuring the healthy development of infants. In this study, we constructed a human milk system containing residual doxycycline (DXC) and/or tetracycline (TC). Machine learning models and clustering algorithms were applied to classify and predict deficient concentrations of single and mixed antibiotics via label-free SERS spectra. The experimental results demonstrate that the CNN model has a recognition accuracy of 98.85% across optimal hyperparameter combinations. Furthermore, we employed Independent Component Analysis (ICA) and the pseudo-Siamese Convolutional Neural Network (pSCNN) to quantify the ratios of individual antibiotics in mixed human milk samples. Integrating the SERS technique with machine learning algorithms shows significant potential for rapid discrimination and precise quantification of single and mixed antibiotics at deficient concentrations in human milk.

1. Introduction

Doxycycline (DXC) and tetracycline (TC) are broad-spectrum antibiotics classified under the group of tetracycline antibiotics (TCs) and are widely used for treating human bacterial infections (Anand, Sivasankaran, Jose, & Kumar, 2019). In clinical settings, the joint use of tetracycline and doxycycline is not usual (Holmes & Charles, 2009). However, due to the widespread use of antibiotics for the treatment of bacterial infections in both humans and animals (Ibraheem & Abdul-Ahad, 2012), excessive antibiotic residues have been found in food products (meat, fish, milk, etc) and contaminated water supplies (Boxall, Kolpin, Halling-Sørensen, & Tolls, 2003). For example, antibiotic residues like tetracycline, chlortetracycline, oxytetracycline, and doxycycline are frequently found in duck meat (T. Wang et al., 2021), pork (De Wasch et al., 1998) and cow milk (Prado, Ferreira, Bando, & Machinski Jr, 2015). The disproportionate use of TCs led to their excessive accumulation in food products and the natural environment, and these residues will finally enter the human body through water and food, endangering human health (Miao, Wang, & Yang, 2018). Antibiotic residues disrupt the delicate microbial balance and contribute to human

* Corresponding author at: Department of Clinical Medicine, School of the 1st Clinical Medicine, Xuzhou Medical University, Xuzhou, Jiangsu Province, China.
** Corresponding author at: Laboratory Medicine, Guangdong Provincial People's Hospital (Guangdong Academy of Medical Sciences), Southern Medical University, Guangzhou, Guangdong Province, China.
E-mail addresses: usman@xzhmu.edu.cn (M. Usman), xylzhao9999@163.com (Z. Liu), healthscience@foxmail.com (L. Wang).
[1] These authors contributed equally to the study.

https://doi.org/10.1016/j.fochx.2024.101507
Received 12 March 2024; Received in revised form 16 May 2024; Accepted 22 May 2024
Available online 24 May 2024

bacterial drug resistance, impacting normal growth processes and causing persistent physiological changes (Mueller & Tronick, 2019). Nursing mothers may consume food products contaminated with these residues during breastfeeding. Therefore, it is essential to identify undesirable toxins and metabolites in human milk that may be passed on to breastfeeding infants. Moreover, infants in their developmental stages may accumulate higher concentrations of these contaminants and experience delayed excretion due to their immature metabolic processes (Mueller & Tronick, 2019; Organization, W. H, 2010). Consequently, it becomes imperative to identify the presence of harmful toxins and metabolites in human milk to prevent their transmission to breastfeeding infants (Dinleyici et al., 2018) .

Numerous studies have evaluated chemical contaminants in human milk and their potential impacts on infants and mothers. Detecting TCs in human milk has garnered significant attention from researchers worldwide due to the associated risks (Z. Xu et al., 2020). However, detecting antibiotics in milk poses challenges owing to the complex matrix composition and low concentrations of target analytes in real-world samples. Hence, developing a sensitive and convenient method for rapid antibiotic quantification would be invaluable for effective control and regulation. Consequently, regulatory authorities have implemented monitoring tests, which have demonstrated significant reductions in the occurrence of milk contaminated with antibiotics (Gajda, Nowacka-Kozak, Gbylik-Sikorska, & Posyniak, 2018; Sivakesava & Irudayaraj, 2002). Microbial inhibition tests, immunoassays, and chemical-physical techniques such as high-performance liquid chromatography or mass spectrometry are widely employed for detecting antibiotic residues. However, these methods entail high operational costs and intricate sample preparation procedures, necessitating substantial volumes of reagents and specialized personnel (Yuan et al., 2024). Furthermore, the number of samples that can be analyzed within a given time frame is limited (Toma, Oishi, Iitani, Arakawa, & Mitsubayashi, 2022).

Surface-enhanced Raman spectroscopy (SERS), known for its exceptional molecular specificity and high sensitivity of substrate materials, has emerged as a valuable tool in various fields, including pathogen detection, cancer diagnosis, and identification of antibiotics in dairy products (Usman et al., 2022; Usman et al., 2023; Wei et al., 2024). In food research, Yang et al. utilized polydimethylsiloxane (PDMS) plasma cavities as SERS substrates to detect tetracycline in milk, achieving a low detection limit of 0.28 μg/L (Z. Yang et al., 2021). Similarly, a study focused on tetracycline residue detection in milk employed silver colloid nanoparticles to prepare mixed solutions of antibiotics and milk with varying concentrations; the concentration of tetracycline was estimated by observing intensity values of characteristic peaks, facilitating qualitative and quantitative detection of tetracycline residues at production sites (Sagar, Kuanglin, Huang, Kim, & Schmidt, 2018). However, most studies have primarily focused on analyzing individual, pure antibiotics within a sample, and the identification and quantification of multiple antibiotics in mixed SERS spectra still need to be improved due to spectral overlap within complex interference backgrounds. Furthermore, applying the SERS approach for precise molecular quantification encounters certain limitations. Manual visual inspection fails to discern minute differences in SERS spectra of antibiotics at varying concentrations, and conventional antibiotic trace detection techniques struggle to detect the vibrational fingerprints of antibiotic molecules. Additionally, Raman signals originating from the blank SERS substrate impede the detection of antibiotics at low concentrations. Consequently, relying solely on the intensity of a single molecular characteristic peak becomes inadequate for concentration differentiation. To address these challenges, machine learning, an advanced statistical method employing multivariate analysis, enables identifying and classifying signal features embedded within large and complex datasets; furthermore, integrating machine learning algorithms with Raman spectroscopy eliminates the subjectivity in determining analyte concentrations based on a single characteristic peak. (Thrift et al., 2020; L. Wang et al., 2022).

Numerous studies have utilized the SERS approach to achieve rapid antibiotic detection (Usman et al., 2019; Usman et al., 2023). Several investigations have been conducted to detect various types of antibiotics using the SERS approach in conjunction with machine learning models (Xie et al., 2012; Z. Xu et al., 2020). However, limited research has focused on using the combined power of the SERS approach and machine learning models to effectively differentiate between antibiotics and to accurately quantify mixed antibiotic concentrations simultaneously. Due to the consumption of food and water products contaminated by antibiotics, co-occurrence of DXC and TC in the human body is possible and these antibiotics can be excreted into human milk with high concentrations (Matsuda, 1984; Niebyl, 2003). Therefore, in this study, we employed a portable Raman spectrometer to collect SERS spectra of doxycycline (DXC) and tetracycline (TC) in human milk samples. These spectra were subsequently analyzed using clustering algorithms and machine learning models to classify and predict single and mixed antibiotics at deficient concentrations. The results demonstrated that human milk samples containing different antibiotics could be rapidly and accurately categorized and predicted. In particular, we employed the Independent Component Analysis (ICA) method and the Pseudo-Siamese Convolutional Neural Network (pSCNN) method to determine the ratios of individual antibiotics. Our findings indicated that the pSCNN algorithm based on SERS technology can successfully quantify the DXC and TC ratios within mixed antibiotic samples. In summary, the proposed machine learning model overcomes the challenges associated with quantitative detection and accurate prediction of mixed antibiotics in human milk. These advancements encourage the development of SERS sensors and their real-world application in this field, which will improve the quality and safety control of human milk and benefit infant health in the near future.

2. Materials and methods

2.1. Chemicals and instruments

Silver nitrate ($AgNO_3$), sodium citrate ($Na_3C_6H_5O_7$), and sulfosalicylic acid were procured from China National Pharmaceutical Group Co., Ltd. (Beijing, China). At the same time, tetracycline and doxycycline were obtained from Sangon Biotech Co. Ltd. (Shanghai, China). All chemicals were used as received without the need for further purification. Human milk samples were collected from a lactating individual at the affiliated hospital of Xuzhou Medical University, with ethical approval and informed consent (Approval Number: XYFY2023-KL169). All magnetic stirring bars and glassware were immersed in aqua regia for 10 h and then triple-rinsed with ultrapure water obtained from a Milli Q-Plus system (Millipore, Bedford, MA, USA).

2.2. Preparation of silver nanoparticles as SERS substrate

Our previous publications have described the synthesis methods for silver nanoparticles (AgNPs) (L. Wang et al., 2022). A triangular flask was employed, and 200 mL of deionized distilled water and 33.72 mg of $AgNO_3$ were added while stirring and heating to boiling. Subsequently, 8 mL of $Na_3C_6H_5O_7$ was added, and the mixture was heated at 120 °C for 40 min at 650 rpm. Afterward, the heating was stopped, and stirring continued until the solution cooled to room temperature. The solution (1 mL) was transferred to a clean Eppendorf (EP) tube and centrifuged at 7000 rpm for 7 min. The supernatant was removed, and the pellet was resuspended in 100 μL of water for long-term storage at room temperature (RT).

2.3. Sample preparation and Raman spectroscopy measurements

Freshly expressed milk from a healthy lactating participant was collected from the Obstetrics and Gynecology Department of the

Affiliated Hospital of Xuzhou Medical University. The 10 mL of milk was centrifuged at 10,000 rpm for 10 min to remove the upper-fat layer. Subsequently, a sulfosalicylic acid solution with a final concentration of 5% was added to the milk, followed by another centrifugation at 10,000 rpm for 10 min to eliminate proteins and polypeptides. The resulting supernatant was then collected for subsequent use. To prepare the stock solutions, 0.9618 mg of tetracycline (TC) and 0.8888 mg of doxycycline (DXC) powder were separately added to 2 mL of the pre-treated human milk supernatant, resulting in a final concentration of 10^{-6} M. Serial dilutions were performed to prepare antibiotic solutions with concentrations of 10^{-6} M, 10^{-7} M, 10^{-8} M, 10^{-9} M and 10^{-10} M. Additionally, a mixed solution of tetracycline and doxycycline with a final concentration of 10^{-9} M was prepared. All samples were sonicated for 10 min to ensure homogeneity.

For Raman spectroscopy measurements, each antibiotic solution at different concentrations was mixed with the AgNPs solution, and the 30 μL mixture was dropped onto a silicon wafer to form circular spots. The spots were then naturally dried in a safety cabinet before detection. Raman spectra were acquired using a portable Anton Paar Cora100™ Raman spectrometer (Anton Paar Shanghai Trading Co., Ltd., China) with the following settings: excitation wavelength of 785 nm, excitation power of 25 mW, spectral resolution of 1 nm, spectral wave number resolution of 10 cm^{-1}, and detection spectral range of 400–2300 cm^{-1}. The Raman peak at 520 cm^{-1} was utilized as the reference peak to calibrate all SERS spectra, and the dark current was subtracted using integration time. 100 spectra were randomly collected from within each dried sample spot, resulting in 600 SERS spectra generated for each sample for further analysis in this study.

2.4. Clustering analysis of SERS spectra

Two clustering algorithms, PCA and OPLS-DA, were employed to investigate the.

inherent differences between the spectra of different saliva samples. Since external factors may influence saliva samples during the collection process, various preprocessing methods were combined with cluster analysis to assess the data quality before cluster analysis. All spectral preprocessing operations were performed using the commercial analysis software Unscrambler X (Version 10.4 64bit, CAMO, Norway). Maximum and minimum normalization was applied to reduce all spectral intensity ranges to the [0,1] range through Maximum normalization. Savitzky-Golay smoothing with a polynomial order of 3 was used for spectral smoothing, and baseline correction was achieved through baseline offset. After each preprocessing step, PCA and OPLS-DA were used for cluster analysis. PCA was implemented using the PCA function in the sci-kit learn (version 0.21.3) data analysis library, with the n_components parameter set to 2 for data fitting. OPLS-DA analysis was performed using the OPLS-DA function in the multivariate statistical analysis software SIMCA (version 13.0, 32-bit) to fit all SERS data of the two types. The clustering results were evaluated using R2X, R2Y, and Q2 indices. These evaluation indices were also used to assess the quality of data preprocessing.

Clustering analysis involves grouping similar SERS spectra into distinct classes to uncover the underlying structures within the spectral data (Aggarwal, 2018; Liu et al., 2023). In this study, two clustering methods, namely Principal Component Analysis (PCA) and Orthogonal Partial Least Squares Discriminant Analysis (OPLS-DA), were employed to analyze the SERS data obtained from human milk samples mixed with three types of antibiotics (DXC, TC, DXC&TC). The PCA method was implemented using the *PCA* function from the Python sci-kit learn package (version 0.21.3). The *fit_transform* method within the *PCA* function was utilized to fit the various SERS signals and perform dimension reduction on the complete set of SERS spectral data. PC1 and PC2, representing the two principal components with the highest contribution values, were selected to capture the overall characteristics of the SERS data. However, as an unsupervised learning algorithm, PCA only uncovers underlying patterns based on data distribution, which can be influenced by factors such as Raman signal intensities and feature shifts. The OPLS-DA, a supervised learning algorithm, was employed to address this limitation. OPLS-DA leverages prior knowledge obtained from data labels to learn specific data patterns and achieve the separation of different SERS signals. In this study, OPLS-DA was conducted using SIMCA software (version 13.0, 32-bit), a commercial multivariate analysis tool, to mitigate the influence of confounding factors on the classification outcomes. Three evaluation indices, namely R2X, R2Y, and Q2, were employed to assess the explanatory and predictive capabilities of the OPLS-DA model.

2.5. Supervised machine learning analysis of SERS spectra

To differentiate and forecast SERS signals of various antibiotics and determine the most effective identification model, this study employed six commonly used machine learning algorithms: Adaptive Boosting (AdaBoost), extreme Gradient Boosting (XGBoost), Linear Discriminant Analysis (LDA), Decision Tree (DT), Random Forest (RF), and Support Vector Machine (SVM). The SERS spectra of two pure antibiotics and mixed antibiotics in human milk were analyzed using these algorithms. The dataset was divided into training, test, and validation sets in a 6:2:2 ratio using the *train_test_split* function from the scikit-learn package (version 0.21.3). To prevent overfitting, each model's training accuracy ($Accuracy_{train}$) was compared with the validation accuracy ($Accuracy_{vali}$) in the training set during the model training processes. The test dataset, independent of the model training, was solely used to assess the performance of each model after training. Before applying different machine learning algorithms to identify spectral data, we optimized the hyperparameters of each model using the *GridSearchCV* function. By setting predetermined ranges for the hyperparameters, we trained each model to obtain the best combination of parameters (**Supplementary Table S1**). After hyperparameter optimization, we performed five-fold cross-validation using the *cv* function, with the parameter set to 5, to assess the robustness of the machine learning models. Throughout the grid search process, we utilized score gradient plots to record the progress and monitored the accuracy and stability of the model during parameter iteration.

2.6. Model performance evaluation

To identify the machine learning model with the best performance, a comprehensive evaluation was conducted using various metrics to compare the performance of different models on the test dataset. The evaluation metrics employed in this study included accuracy (ACC), precision (Pre), recall (Re), and F1-score (F1). These metrics encompass four distinct scenarios: True Positive (TP), True Negative (TN), False Positive (FP), and False Negative (FN). The *accuracy_score function* was utilized to calculate the ACC score, providing an overview of correct predictions across all outcomes. To address any imbalances in dataset splitting, the *precision_score* and *recall_score* functions were employed to measure the model's ability to identify samples with actual values. As precision and recall are mutually exclusive, the F1-score, calculated using the *f1_score* function, served as the harmonic average of the two metrics, offering a measure of the model's proficiency in identifying true values. A 5-fold cross-validation approach was adopted to mitigate model overfitting, dividing the dataset into five subsets. One subset was selected as the validation set, while the remaining four subsets were used for training. This process was repeated five times, and the average value was considered the final evaluation score. Furthermore, to optimize computational resources and obtain highly accurate and efficient identification models, the training times of different models were compared using the *time* function to record the duration of the training process. Models that consumed less time during training required lower computational resources, aligning with our objectives.

2.7. Ratio quantification in human Milk with mixed antibiotics

2.7.1. Independent component analysis

To observe the linear combination of independent components in mixed antibiotic SERS signals and achieve maximum independence among different antibiotic signal components, this study employed the *FastICA* function in the sci-kit learn library (version 0.21.3) for blind-source separation of SERS signals from mixed antibiotics in human milk samples. During the analysis, we included different numbers of n_component (NC) from 2 to the maximum number and determined the optimal NC via ICA_by_blocks (Boiret, Rutledge, Gorretta, Ginot, & Roger, 2014). Each IC loading was denoted as ICx/NCy, where x represents the range [1, y], and y corresponds to the value of NC. The implementation of all loadings was carried out using the *components_* function in FastICA. Subsequently, the correlation between these IC loadings and each reference spectrum was calculated using the Pearson function from the Scipy data analysis package (version 1.4.1) to identify the compounds in the mixture. The IC loading with the highest correlation was recorded and repeated until all reference spectra were compared.

2.7.2. Pseudo-Siamese convolutional neural network (pSCNN)

As ICA cannot discern the proportion of components in the mixture, the Pseudo-Siamese Convolutional Neural Network (pSCNN) was introduced to characterize the SERS signal of the mix. This network consists of two sub-network structures which do not share the training weight. These sub-networks extract features from the Raman spectrum using convolutional layers. Due to the involvement of mixtures and pure compounds in the model training, using a network with shared weights to extract feature vectors is unsuitable. During the network training, the weights of each subnetwork are trained separately, ensuring there is no weight sharing between the two subnetworks. The learned feature vectors are input into dense layers to identify whether there is a containment relationship between the two inputs, thereby achieving compound identification in the SERS spectra of mixtures. The network structure primarily comprises an input layer, convolutional layer, Batch Normalization layer, Maxpooling layer, and dense layer. Unlike a regular convolutional neural network, the input of the pSCNN is a pair of SERS spectra categorized as follows: 1 represents a pure antibiotic, 0.1 represents a mixture of antibiotics containing the pure compound, and 0 represents the spectrum of a pure antibiotic or a mixture of antibiotics not containing that pure compound. Upon inputting the spectral pair into the pSCNN network, the convolutional layers of the two sub-networks independently extract signal features. Each convolutional layer consists of 32 kernels with a size of 3*1, and a *relu* activation function is applied to introduce non-linear relationships between network structures. The BatchNormalization layer is employed to accelerate model training and prevent overfitting. A Maxpooling layer is utilized to reduce the dimensionality of feature maps and enhance translation invariance, with a *pool_size* set to 3. Finally, the feature vectors are fed into the last dense layer, which combines advanced features extracted from the leading body network in a non-linear manner to determine the presence of an inclusion relationship between the spectrum of unknown mixed antibiotics and the spectrum of a single antibiotic. The *Sigmoid* activation function provides the probability of the components present in the mixture, enabling the recognition of single antibiotics within the SERS spectrum of the mix.

3. Result and discussions

3.1. Workflow of trace antibiotic detection

This study subjected human milk to a mixture of DXC and TC antibiotics. The aim was to establish the detection limit for the lowest concentration by generating label-free SERS spectra for each antibiotic and its combination. Clustering analysis was employed to gain an initial understanding of the spectral sample distributions. Furthermore, six classical machine learning algorithms (AdaBoost, LDA, DT, RF, SVM, and XGB) were utilized to identify the three antibiotic combinations. To ascertain the mixed ratio of antibiotics, pSCNN was employed. This method involved dissecting the SERS spectrum of the mixture and providing a schematic representation, which indicated the proportion of each antibiotic. Applying SERS sensors directly to real-world samples like human milk presents challenges due to interfering compounds (Fang et al., 2022). It should be noted that, in this experiment, human milk underwent centrifugation with acid to eliminate fat and protein, and the resulting supernatant was collected for SERS spectral detection.

3.2. SERS reproducibility and uniformity

In specificity, the SERS spectra of the two antibiotics DXC and TC in human milk were generated and demonstrated with concentrations ranging from 10^{-6} to 10^{-10} M, separately and jointly (Fig. 1A-B). According to the previous report, following an oral dosage of 200 mg of DXC, the concentration of DXC in human milk can reach 0. 38 mg/L, which is equivalent to 8.24×10^{-7} M; in addition, after orally taking 150 mg tetracycline, the peak concentration of TC in human milk was 0.8 mg/L, which corresponds to 1.8×10^{-6} M (Matsuda, 1984; Niebyl, 2003). In this study, our approach's detection limit equals to 10^{-9} M for both doxycycline and tetracycline. Therefore, our method is able to provide sufficient sensitivity for the detection of the two antibiotics in human milk. It is worth noting that various techniques have also been reported for antibiotic detection in different milk samples for comparative study (Table 1). In these studies, DXC and TC are detected in cow, ovine, and whole milk, but in our work. The major drawbacks of these methods are the long measuring time and the requirement for special pretreatment of the milk samples. In contrast, our SERS approach requires no special treatment of either milk or TCs, enabling direct and label-free detection at low concentration levels with shorter measuring times.

The DXC spectra exhibited primary characteristic peaks at 1316 cm^{-1} and 1628 cm^{-1}, while the TC spectrum displayed primary characteristic peaks at 1268 cm^{-1} and 1616 cm^{-1}. Specifically, the 1316 cm^{-1} peak in DXC was attributed to the rocking of C1-H33 and C8-H34, while the 1628 cm^{-1} band originated from the symmetric stretching of C21-C28 and the bending of C29-O32-H57. On the other hand, the 1268 cm^{-1} peak in tetracycline resulted from the amide triple doublet, and the 1616 cm^{-1} peak was attributed to C═O stretching vibrations. Previous literature has compared the SERS spectra of antibiotics in raw milk to assess the impact of centrifugally filtered human milk on the SERS spectra of antibiotics (Pinheiro, Fateixa, Nogueira, & Trindade, 2018; Tackman et al., 2018). The results confirmed the emergence of new characteristic peaks in the SERS spectra of antibiotic samples in human milk compared to those in raw milk. Thus, the human milk solution exhibited more distinct and pronounced characteristic antibiotic peaks, facilitating spectral analysis. To assess the reproducibility of the DXC SERS spectra, a comprehensive statistical analysis was conducted to quantify the variations in SERS signal intensity across different spot-to-spot measurements (P. Li et al., 2016). The SERS intensity's relative standard deviation (RSD) was determined for the 1218 cm^{-1}, 1316 cm^{-1}, and 1628 cm^{-1} peaks of DXC, based on 100 randomly selected spots, as depicted in Fig. 1C. The calculated RSD values for these peaks were 7.66%, 7.84%, and 8.32%, respectively.

Similarly, for TC, the SERS performance of the substrate was evaluated by measuring the intensity of 1238 cm^{-1}, 1314 cm^{-1}, and 1614 cm^{-1} peaks at 100 different random spots, yielding RSD values of 8.12%, 8.82%, and 8.624%, as illustrated in Fig. 1D (Perales-Rondon, Colina, Gonzalez, & Escarpa, 2020). These results confirm the reproducibility of the proposed SERS approach in practical and biological contexts. Consequently, these findings demonstrate the feasibility of the approach, which exhibits excellent accuracy and reproducibility for detecting trace antibiotics in real-world human milk samples. Moreover,

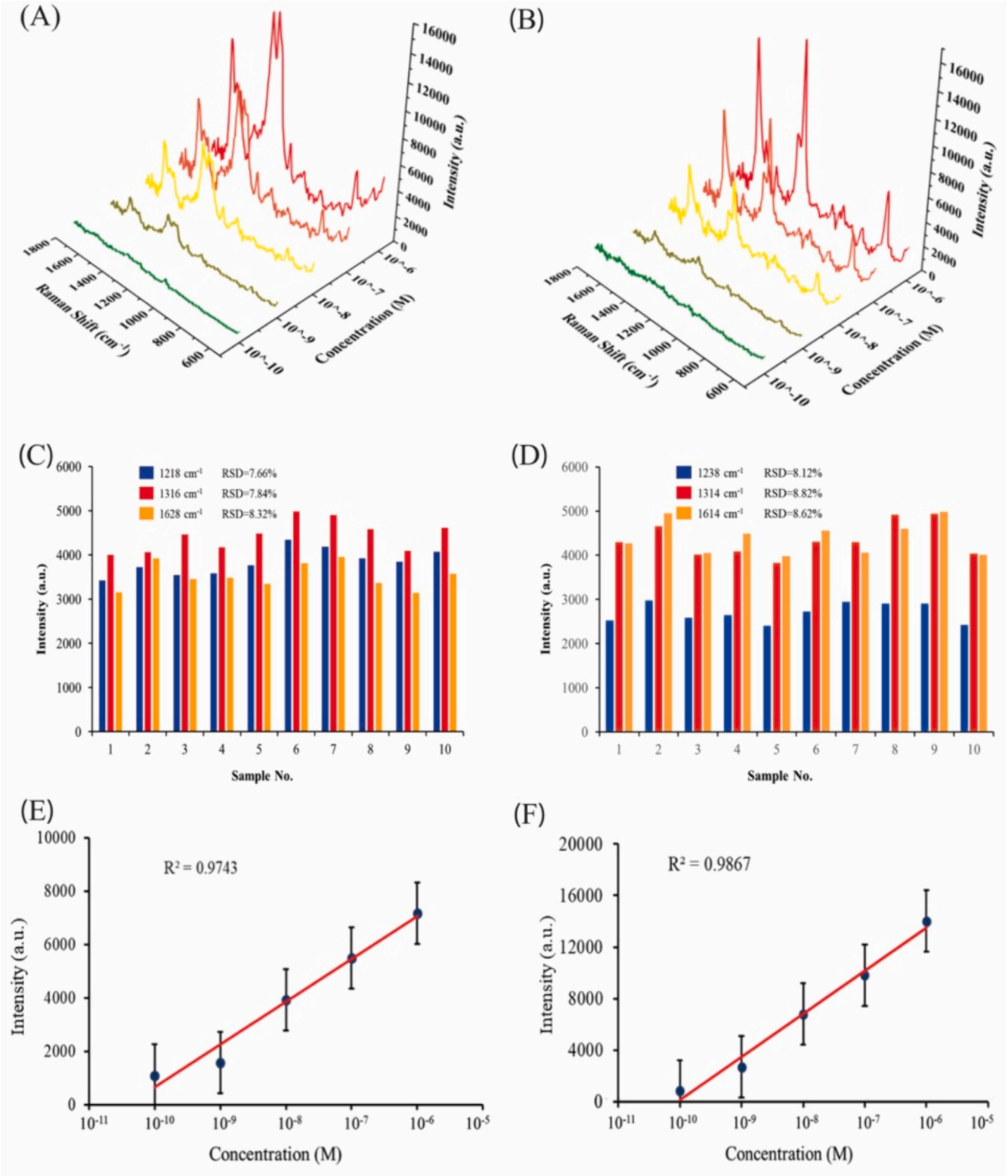

Fig. 1. Detection and quantitation of DXC and TC in human milk. Panels (A-B) display the SERS spectra of DXC and TC in milk, presenting different concentrations ranging from 10^{-6} M to 10^{-10} M. The histograms in panels (C—D) illustrate the distribution of the peak SERS intensity for major peaks of DXC and TC acquired from random spots on the SERS substrate. Panels (*E*-F) depict the linear correlation between the concentrations of DXC and TC in human milk and the SERS signal intensity at 1620 cm^{-1}.

calibration curves were generated for the characteristic Raman peaks of DXC and TC, plotting the intensity-concentration relationship, as presented in Fig. 1**E** and **F**, respectively. The calibration curve was constructed using distinct peaks at various concentrations, with 100 repeated experiments for each concentration. A strong linear correlation was observed between the SERS signal and concentration ratio, with correlation coefficients of $R2_{DXC} = 0.9743$ and $R2_{TC} = 0.9868$. Overall, the comparative findings demonstrate that the SERS approach employed

Table 1
Comparison of various methods employed for detecting TC and DXC in different milk samples and the limit of detection (LOD).

Methods	Antibiotics	Matrix	LOD	Refs.
Colorimetric	Tetracycline	Cow milk	266 pM	(Ramezani, Danesh, Lavaee, Abnous, & Taghdisi, 2015)
HPLC	Tetracycline	Bovine milk	0.95–3.6 μg/L	(H. Xu et al., 2017)
ELISA	Tetracycline	Cow milk	3.30 μg kg^{-1}	(Du et al., 2019)
Fluorescent	Tetracycline	Cow milk	45 ng/mL	(Ahmed, Kumar, Ortega, Srinivasan, & Rajabzadeh, 2021)
ECL	Tetracycline	Cow milk	0.0053 ng/mL	(R. Xu et al., 2023)
HPLC	Doxycycline	Ovine milk	0.06 μg/mL	(Mileva, 2019)
ELISA	Doxycycline	Whole cow milk	0.1 μg/L	(Adrian, Fernandez, Sanchez-Baeza, & Marco, 2012)
Capillary	Doxycycline	Cow milk	0.0808 μg/mL	(Mu, Liu, Xu, Tian, & Luan, 2012)
Fluorescence	Doxycycline	Cow milk	47 nM	(Yu et al., 2020)
SERS	Doxycycline Tetracycline	Human milk	10^{-10} M	This work

in this study enables rapid and label-free detection of antibiotics in human milk at low concentrations compared to conventional methods.

3.3. SERS spectral characteristic peaks analysis

To further explore the practical application of this approach, we investigated the distinctions among the characteristic peaks of various antibiotics. Consequently, we devised a method for detecting spectral mixtures based on these distinct peaks. We can identify the characteristic peaks corresponding to individual antibiotics within the mixture by analyzing the Raman spectrum of mixed antibiotics. These typical values are marked in Fig. 2 to aid in analyzing variations among different spectral mixtures. Specifically, a mixture solution was created by combining equal volumes of DXC and TC at a concentration of 10^{-9} M, and a small quantity of AgNPs was introduced into the solution to monitor the vibrational modes of DXC and TC (Fig. 2A-C). The experimental frequencies and assignments for DXC, TC, and the mixed solution are presented in Fig. 2D-F. The collected spectra revealed several notable peaks for DXC (1172, 1248, 1276, 1450, 1748, 1776 cm^{-1}) and TC (1052, 1314, 1482, 1616, 1748, 1776 cm^{-1}). Our study's results demonstrate the efficacy of our method in producing consistent spectra from various surface locations. Moreover, our method can distinguish between antibiotic contaminants in human milk samples. These findings highlight our approach's potential for accurately identifying and differentiating contaminants.

3.4. Cluster analysis of SERS spectra of different antibiotics

Clustering analysis, as highlighted by Jain, Murty, and Flynn (1999), is a valuable tool for identifying commonalities within datasets. Thus, in this study, two clustering algorithms, namely PCA and OPLS-DA, were employed to perform clustering analysis on the SERS signals. The outcomes of the unsupervised learning PCA algorithm revealed a considerable overlap among the sample points of the three antibiotic SERS spectra, indicating relatively indistinct clusters and a suboptimal performance of the PCA algorithm on this particular dataset (Fig. 3A). Conversely, OPLS-DA, a supervised multivariate statistical approach for data clustering, provided insights into the divisions of data groups based on high-dimensional spectral measurements. The results obtained from OPLS-DA exhibited well-defined clustering of the three antibiotic spectra into distinct groups, characterized by reduced intra-genus variations and clear boundaries between the groups (Fig. 3B). Furthermore, the evaluation indices, R2X = 0.971, R2Y = 0.903, and Q2 = 0.88, demonstrated the proficiency of OPLS-DA in effectively distinguishing different SERS signals.

3.5. Optimization of machine learning model parameters

Consistency and optimization of machine learning parameters are crucial due to the varying performance they can exhibit across different

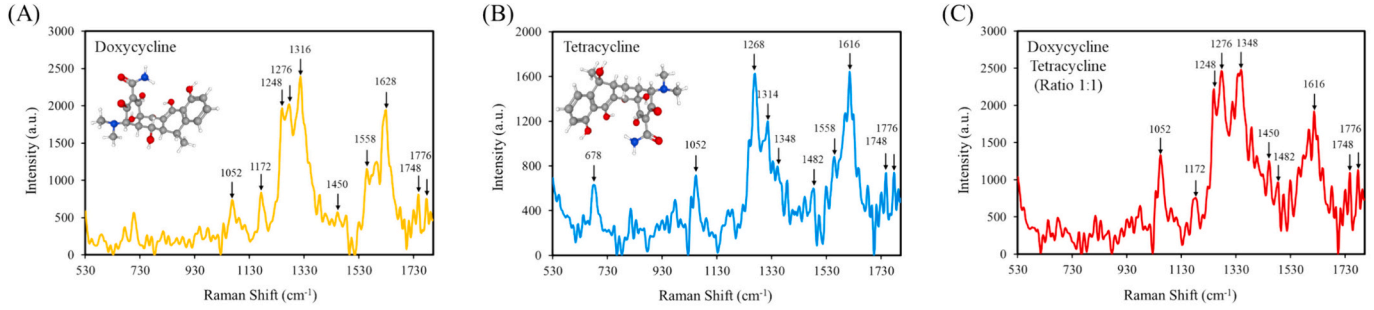

(D)

Wavenumber (cm^{-1})	Band Assignment
1052	*ν* (C-C)
1172	str C_2-C_5, rock C_{30}-H_{55}
1248	stretching C-N
1276	breath ring $C_8C_{11}C_{19}C_{24}C_{21}C_{15}$
1316	Rock C_1-H_{33}, rock C_8-H_{34}
1450	Bend C_{29}-O_{32}-H_{57}, rock C_{28}-H_{54}
1558	sciss $N_{26}H_2$
1628	sym str C_{21}-C_{28}, bend C_{29}-O_{32}-H_{57}
1748	C=O
1776	Aged oil drying

(E)

Wavenumber (cm^{-1})	Band Assignment
678	Ring-breathing II model solid melamine
1052	*ν* (C-C)
1268	amide III doublet
1314	Rock C_1-H_{33}, rock C_8-H_{34}
1482	stretch vibration of furan ring
1558	sciss $N_{26}H_2$
1616	C=O stretching vibration
1748	C=O
1776	Aged oil drying

(F)

Wavenumber (cm^{-1})	Antibiotics
1052	Doxy/Tetra
1172	Doxy
1248	Doxy
1276	Doxy
1348	Tetra
1450	Doxy
1482	Tetra
1616	Tetra
1748	Doxy/Tetra
1776	Doxy/Tetra

Fig. 2. Average SERS spectra and characteristic peaks of single and mixed antibiotics in human milk. (A) Average SERS spectrum representing doxycycline. (B) Average SERS spectrum representing tetracycline. (C) Average SERS spectrum of mixed antibiotics. (D—F) Characteristic peaks in the SERS spectra and biological significance.

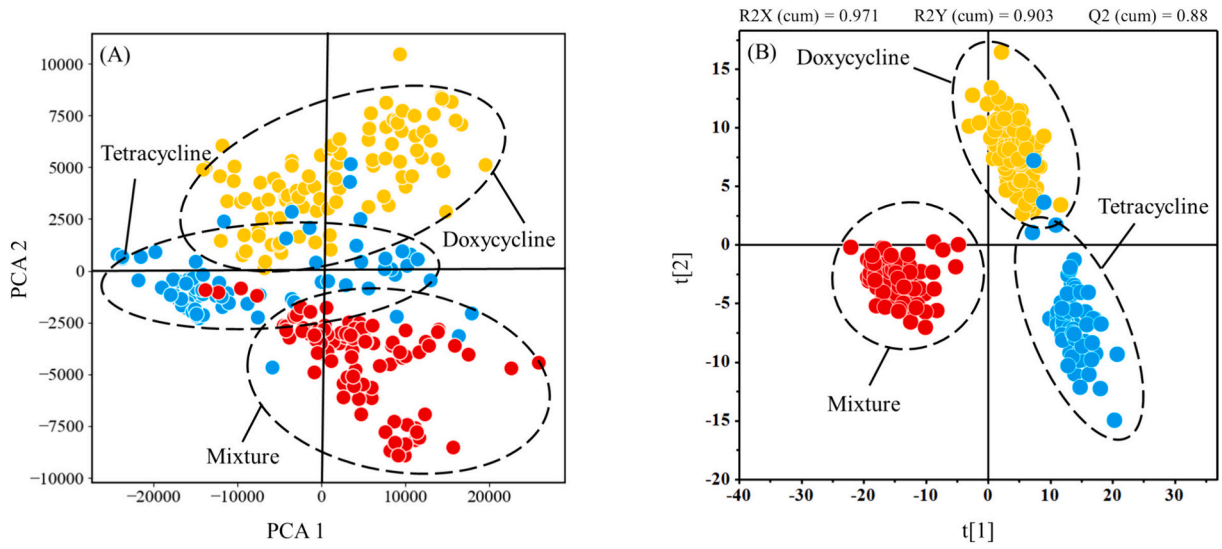

Fig. 3. Clustering analysis of SERS spectra of human milk samples with single and mixed antibiotics using PCA and OPLS-DA algorithms. (A) PCA Analysis: The scatter plot of sample points shows a relatively dispersed distribution. (B) OPLS-DA Analysis. Distinct clusters are formed as different sample points are grouped into separate clusters.

datasets, sometimes even displaying contrasting outcomes (L. Yang & Shami, 2020). Therefore, it is essential to optimize model parameters before data analysis. In this study, we employed a grid search approach to optimize the hyperparameters of six machine learning algorithms, and the resulting grid search gradient plots were used to showcase the learning capability and stability of these algorithms. The findings demonstrated that Support Vector Machine (SVM) consistently achieved the highest recognition accuracy (ACC = 98.85%) across all hyperparameter combinations (Fig. 4A). This result indicates that the SVM algorithm possesses exceptional analytical capabilities for high-dimensional data with limited sample sizes, which aligns with previous studies (Liu et al., 2023). Linear discriminant analysis (LDA) achieved performance similar to SVM; however, fluctuations in training accuracy were observed across different parameter combinations, as depicted in the fitting results in Fig. 4B. Only when the shrinkage parameter size was set to 0.01 did the algorithm's accuracy exceed 0.98. Moreover, Random Forest (RF) with parameters (criterion = 'gini', max_depth = 8, n_estimators = 90) in Fig. 4C, XGBoost with parameters (learning_rate = 0.1, n_estimators = 120) in Fig. 4D, and Decision Tree (DT) with parameters (criterion = 'entropy', max_depth = 29, max_features = 26) in Fig. 4E also identified the optimal parameter combinations for recognition accuracy through the grid search process, The recognition accuracy for all these algorithms exceeded 90%. Conversely, the AdaBoost algorithm exhibited the lowest performance among all the algorithms, achieving recognition accuracy above 0.9 only when the parameter learning_rate was set to 0.1 (Fig. 4F).

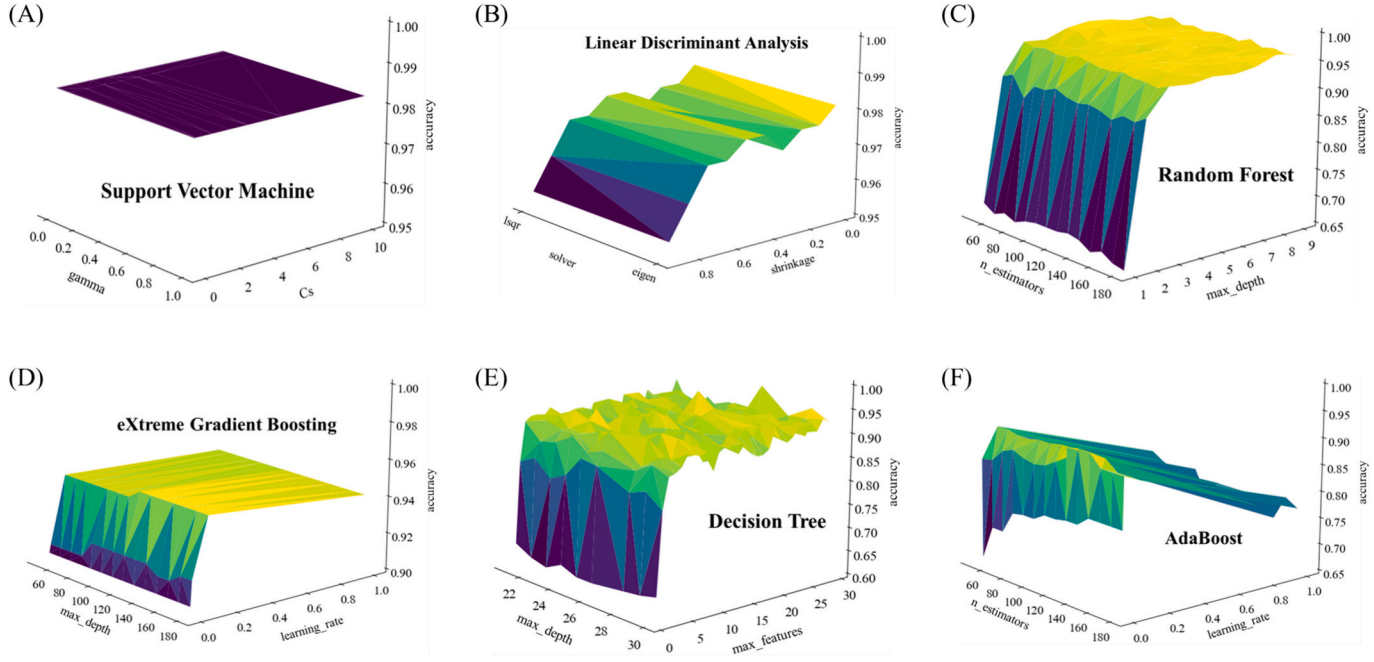

Fig. 4. Parameter optimization of six machine learning algorithms. (A) Support Vector Machine., (B) Linear Discriminant Analysis, (C) Random Forest, (D)eXtreme Gradient Boosting, (E) Decision Tree, and (F) AdaBoost.

3.6. Evaluation of machine learning model performance

The hyperparameters were adjusted and updated using both the training and validation datasets. However, it is well-known that evaluation metrics can often be overly optimistic. To honestly assess the model's performance on unseen samples, an independent test set was utilized for performance evaluation (Table 2). According to the results, the SVM model exhibited the best performance among all algorithms, with all metrics surpassing 98%. Additionally, the SVM model demonstrated the second shortest model fitting time (Time = 0.053 s) compared to other algorithms. These findings indicate that SVM efficiently and reliably analyzes different SERS data. LDA achieved similar scores to SVM across all evaluation metrics, suggesting that LDA could also serve as a potential method for recognizing SERS signals. The remaining algorithms achieved recognition accuracy of over 90%. Notably, the XGBoost algorithm had the highest computational resource utilization, with a fitting time of 2.11 s. On the other hand, the DT algorithm exhibited the shortest reasonable time of only 0.004 s, suggesting its ability to swiftly discriminate SERS signals of different antibiotics. However, the DT algorithm's recognition accuracy was only 92.73%.

3.7. Identification of compounds in mixtures using ICA

In many instances, identifying biological samples poses a challenge due to mixed antibiotics. The complexity arises from the overlapping and interfering signals of multiple antibiotics in the SERS signal, making it difficult to determine the composition and ratio of the mixed samples (Dina et al., 2022). To address this issue, we employed the Independent Component Analysis (ICA) method to discern individual antibiotics within the SERS spectrum of the mixture. By computing and comparing the correlation coefficients of IC loadings with all NCs, we selected the top two IC loadings highly correlated with the reference spectra of the two antibiotics for presentation. For Doxycycline (Fig. 5A), the optimal two IC loadings were IC01/NC02 and IC07/NC07, with correlation coefficients of 76.24% and 59.49%, respectively (Fig. 5B). This indicates that ICA can only partially deconvolute pure antibiotics. Similarly, in the analysis of Tetracycline (Fig. 5C), the best two IC loadings were IC01/NC02 and IC03/NC04, with correlation coefficients of 73.57% and 56.98%, respectively (Fig. 5D). This result contrasts with previous findings suggesting that ICA can accurately identify target antibiotics in mixtures (Limwichean et al., 2023). This reduced correlation suggests that the signal of antibiotics may be influenced by either the substrate background or the interaction between the compounds, particularly as the concentration of the mixture decreases (Limwichean et al., 2023). ss.

3.8. Identification of compounds in mixtures using pSCNN

Due to the limitations of the Independent Component Analysis (ICA) method, the pSCNN algorithm was employed in this study to determine the proportions of individual antibiotics in the mixture. To evaluate the identification performance of pSCNN on real-world SERS spectra, the known content of the single antibiotic component in the mixture spectrum was preset in the antibiotic database. The test dataset, consisting of mixture spectra not included in the model training, was then used for verification. Ten SERS spectrum data points were extracted and input into the model to predict the proportions of single antibiotics within the mixture. As illustrated in Fig. 6, the pSCNN model successfully maintained the ratio of the two elemental antibiotics within the range of 0.4–0.6 across the ten unknown mixture spectra. Notably, the prediction ratios for mixture spectra 6 and 8 almost reached a 1:1 proportion. These findings confirm the robust performance of the pSCNN model in accurately identifying the components within the mixture.

3.9. Limitations and future perspectives

The application prospects of Raman spectroscopy in detecting trace antibiotics are considerable. However, most current research is still in the experimental stage, and before this technology can replace traditional detection methods, several existing challenges need to be overcome. The preparation of SERS active substrates is the basis for the development of SERS technology in the analysis of milk, body fluids, or water (He, Sun, Pu, Chen, & Lin, 2019). The SERS active substrates developed in this study are mainly derived from nano-silver colloids, which are simple to prepare and cost-effective. However, silver/gold substrates are particularly susceptible to oxidation in air, greatly reducing the SERS enhancement effect. Therefore, SERS substrates with strong signal enhancement and good antioxidative properties are needed. Currently, Ag SHIN monolayer (J. L. Yang et al., 2017), cyclodextrin-decorated Ag NPs (Ma et al., 2013), and Ni/Au core-shell MPs (R. Li, Zhang, Chen, Yan, & Wang, 2011) have been proposed. Secondly, similar to this study, most current research covers few types of antibiotics, and there is limited availability of high-quality public SERS data, with variations in laser wavelength, laser power, and exposure time used for spectrum acquisition. Therefore, more research is needed to accumulate a database of trace antibiotics in liquids with high recognition rates. Additionally, in this study, normalization was performed on all data before using pSCNN analysis. Although this operation effectively improved the fitting speed and recognition accuracy of the model, the baseline and noise levels of low-concentration component samples may be amplified after normalization (Fan et al., 2023), which may degrade the performance of pSCNN when processing spectra of mixtures of multiple (more than two) low-concentration antibiotics. To address this, we need to develop better normalization algorithms and recognition models to improve the accuracy of Raman spectral identification of weak characteristic peaks.

4. Conclusion

This study presents a comprehensive analysis of TC and DXC residues in human milk samples using SERS in combination with computational methods. The study demonstrates a strong linear correlation between the concentrations of TC and DXC residues and the intensity of SERS signals. In order to develop an optimal intelligent detection method, the study explores the application of machine learning algorithms to differentiate and predict SERS spectra generated from human milk samples containing different antibiotics. Among all the machine learning algorithms, SVM consistently demonstrates the highest prediction accuracy (ACC = 98.85%), indicating its effectiveness in analyzing trace antibiotics in human milk. Additionally, to quantify the

Table 2
Performance Comparison of Six Supervised Machine Learning Algorithms in Predicting SERS Spectra of Three Antibiotics in Human Milk.

Algorithm	Accuracy	Precision	Recall	F1-score	5-Fold	Time
SVM	**98.85%**	**98.85%**	**98.24%**	**98.85%**	**98.14%**	**0.053 s**
LDA	98.18%	98.18%	97.44%	98.17%	97.19%	0.16 s
RF	96.36%	96.36%	96.10%	96.36%	95.83%	0.214 s
XGBoost	94.55%	94.55%	94.77%	94.52%	94.94%	2.11 s
DT	92.73%	92.73%	90.97%	92.53%	90.72%	0.004 s
AdaBoost	90.91%	90.91%	92.10%	90.98%	92.68%	1.82 s

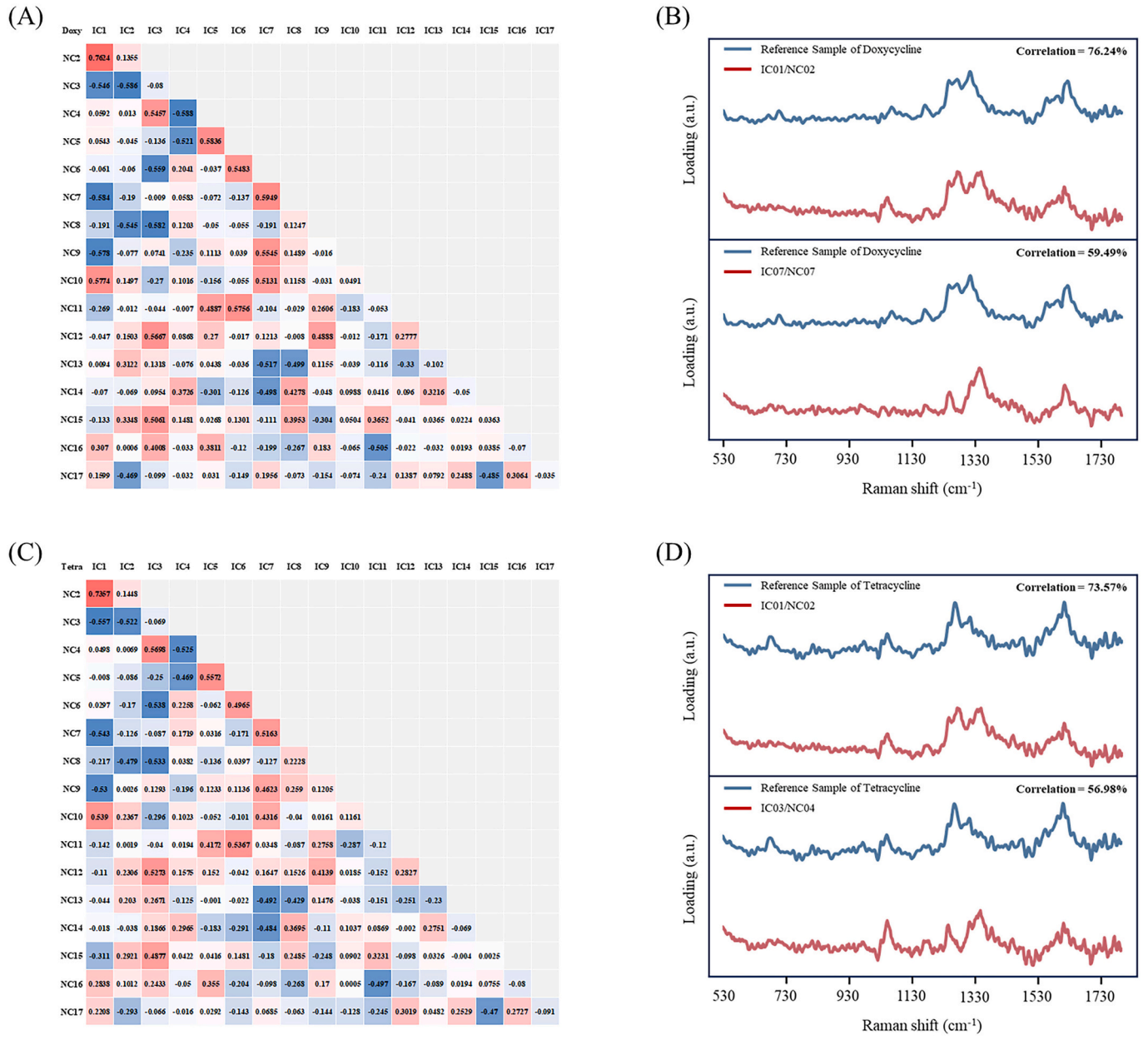

Fig. 5. IC loadings obtained from SERS spectra of human milk containing mixed antibiotics at a concentration of 10^{-9} M. (A) IC loading correlation heatmap for doxycycline. (B) Top two IC loading for doxycycline. (C) IC loading correlation heatmap for tetracycline. (D) Top two IC loading for tetracycline.

proportions of various antibiotics in mixed breast milk samples, the pSCNN algorithm was employed to effectively identify pure substances in mixed antibiotic spectra. In conclusion, the study highlights the potential of a machine learning-enabled Raman spectral identification approach for rapid and reliable detection of antibiotics and quantification of their ratios in human milk samples. This approach holds promise for real-world applications and can contribute to ensuring the safety and quality of human milk products.

5. Publisher's note

All claims expressed in this article are solely those of the authors and do not necessarily represent those of their affiliated organizations or those of the publisher, the editors, and the reviewers. Any product that may be evaluated in this article or claim made by its manufacturer is not guaranteed or endorsed by the publisher.

Authors contributions

LW and ZL designed the experiments, provided the platform and resources for the project, and were responsible for project administration. JYM, MU, JWT, QY, ZWM, and XRW conducted the experimental work. JYM, MU, JWT, and QY performed data analysis and data visualization. All the authors wrote and revised the manuscript. All the authors read and approved the final manuscript.

Funding Statement

Dr. Liang Wang appreciated the financial support of the Guangdong Basic and Applied Basic Research Foundation [No. 2022A1515220023] and the Research Foundation for Advanced Talents of Guangdong Provincial People's Hospital [Grant No. KY012023293].

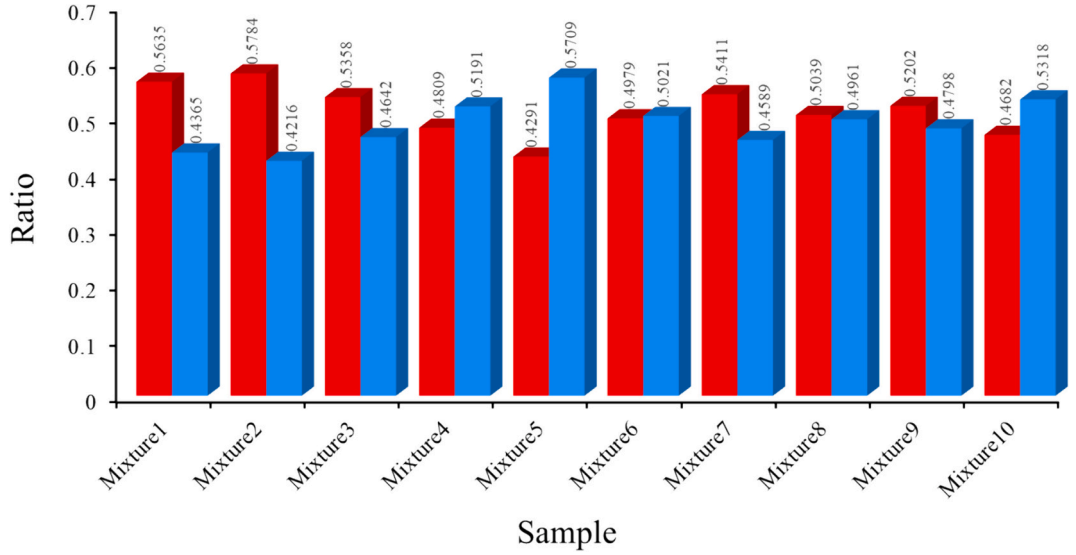

Fig. 6. Prediction performance of pSCNN in the ratio of mixed antibiotics. The figure showcases the results obtained from the pSCNN model, where the red column represents doxycycline, and the blue column represents tetracycline. The pSCNN model was employed to predict the proportions of these antibiotics within the mixture. (For interpretation of the references to colour in this figure legend, the reader is referred to the web version of this article.)

CRediT authorship contribution statement

Jing-Yi Mou: Writing – original draft, Visualization, Validation. **Muhammad Usman:** Writing – original draft, Visualization, Validation. **Jia-Wei Tang:** Writing – original draft, Visualization, Validation. **Quan Yuan:** Validation, Data curation, Conceptualization. **Zhang-Wen Ma:** Validation, Conceptualization. **Xin-Ru Wen:** Validation, Formal analysis. **Zhao Liu:** Supervision, Methodology, Investigation. **Liang Wang:** Writing – review & editing, Supervision, Resources, Methodology, Investigation, Funding acquisition.

Declaration of competing interest

The authors declare that they have no known competing financial interests or personal relationships that could have appeared to influence the work reported in this paper.

Data availability

Data will be made available on request.

Acknowledgments

We thank the anonymous reviewers for their insightful comments that significantly improve the quality of this manuscript.

Conflict of interest

The authors declare that the research was conducted without any commercial or financial relationships that could be construed as a potential conflict of interest.

Appendix A. Supplementary data

Supplementary data to this article can be found online at https://doi.org/10.1016/j.fochx.2024.101507.

References

Adrian, J., Fernandez, F., Sanchez-Baeza, F., & Marco, M.-P. (2012). Preparation of antibodies and development of an enzyme-linked immunosorbent assay (ELISA) for the determination of doxycycline antibiotic in milk samples. *Journal of Agricultural and Food Chemistry, 60*(15), 3837–3846.

Aggarwal, C. C. (2018). An introduction to cluster analysis. In *Data Clustering* (pp. 1–28). Chapman and Hall/CRC.

Ahmed, S. R., Kumar, S., Ortega, G. A., Srinivasan, S., & Rajabzadeh, A. R. (2021). Target specific aptamer-induced self-assembly of fluorescent graphene quantum dots on palladium nanoparticles for sensitive detection of tetracycline in raw milk. *Food Chemistry, 346*, Article 128893.

Anand, S. K., Sivasankaran, U., Jose, A. R., & Kumar, K. G. (2019). Interaction of tetracycline with l-cysteine functionalized CdS quantum dots-fundamentals and sensing application. *Spectrochimica Acta Part A: Molecular and Biomolecular Spectroscopy, 213*, 410–415.

Boiret, M., Rutledge, D. N., Gorretta, N., Ginot, Y.-M., & Roger, J.-M. (2014). Application of independent component analysis on Raman images of a pharmaceutical drug product: Pure spectra determination and spatial distribution of constituents. *Journal of Pharmaceutical and Biomedical Analysis, 90*, 78–84.

Boxall, A. B., Kolpin, D. W., Halling-Sørensen, B., & Tolls, J. (2003). Peer reviewed: Are veterinary medicines causing environmental risks? *Environmental Science & Technology, 37*(15), 286A–294A.

De Wasch, K., Okerman, L., De Brabander, H., Van Hoof, J., Croubels, S., & De Backer, P. (1998). Detection of residues of tetracycline antibiotics in pork and chicken meat: Correlation between results of screening and confirmatory tests. *Analyst, 123*(12), 2737–2741.

Dina, N. E., Tahir, M. A., Bajwa, S. Z., Amin, I., Valev, V. K., & Zhang, L. (2022). SERS-based antibiotic susceptibility testing: Towards point-of-care clinical diagnosis. *Biosensors and Bioelectronics, 291*, 1–12.

Dinleyici, M., Yildirim, G., Aydemir, O., Kaya, T., Bildirici, Y., & Carman, K. (2018). Human milk antibiotic residue levels and their relationship with delivery mode, maternal antibiotic use and maternal dietary habits. *European Review for Medical and Pharmacological Sciences, 22*(19), 6560–6566.

Du, B., Wen, F., Guo, X., Zheng, N., Zhang, Y., Li, S., & Xu, Q. (2019). Evaluation of an ELISA-based visualization microarray chip technique for the detection of veterinary antibiotics in milk. *Food Control, 106*, Article 106713.

Fan, X., Wang, Y., Yu, C., Lv, Y., Zhang, H., Yang, Q., & Zhang, Z. (2023). A universal and accurate method for easily identifying components in Raman spectroscopy based on deep learning. *Analytical Chemistry, 95*(11), 4863–4870.

Fang, G., Lin, X., Liang, X., Wu, J., Xu, W., Hasi, W., & Dong, B. (2022). Machine learning-driven 3D Plasmonic cavity-in-cavity surface-enhanced Raman scattering platform with triple synergistic enhancement toward label-free detection of antibiotics in Milk. *Small, 18*(45), 2204588.

Gajda, A., Nowacka-Kozak, E., Gbylik-Sikorska, M., & Posyniak, A. (2018). Tetracycline antibiotics transfer from contaminated milk to dairy products and the effect of the skimming step and pasteurisation process on residue concentrations. *Food Additives & Contaminants: Part A, 35*(1), 66–76.

He, H., Sun, D.-W., Pu, H., Chen, L., & Lin, L. (2019). Applications of Raman spectroscopic techniques for quality and safety evaluation of milk: A review of recent developments. *Critical Reviews in Food Science and Nutrition, 59*(5), 770–793.

Holmes, N. E., & Charles, P. G. (2009). Safety and efficacy review of doxycycline. *Clinical Medicine Insights: Therapeutics, 1*, 471–482.

Ibraheem, J. A., & Abdul-Ahad, M. Y. (2012). Detection of tetracycline, doxycycline, chlortetracycline, and oxytetracycline antibiotics in Nineveha drug wastewater. *Al-Nahrain Journal for Engineering Sciences, 15*(2), 215–221.

Jain, A. K., Murty, M. N., & Flynn, P. J. (1999). Data clustering: A review. *ACM computing surveys (CSUR), 31*(3), 264–323.

Li, P., Li, Y., Zhou, Z. K., Tang, S., Yu, X. F., Xiao, S., & Wang, H. (2016). Evaporative self-assembly of gold nanorods into macroscopic 3D plasmonic superlattice arrays. *Advanced Materials, 28*(13), 2511–2517.

Li, R., Zhang, H., Chen, Q.-W., Yan, N., & Wang, H. (2011). Improved surface-enhanced Raman scattering on micro-scale au hollow spheres: Synthesis and application in detecting tetracycline. *Analyst, 136*(12), 2527–2532.

Limwichean, S., Leung, W., Sataporncha, P., Houngkamhang, N., Nimittrakoolchai, O.-U., Saekow, B., & Botta, R. (2023). Label free detection of multiple trace antibiotics with SERS substrates and independent components analysis. *Spectrochimica Acta Part A: Molecular and Biomolecular Spectroscopy, 295*, Article 122584.

Liu, W., Tang, J.-W., Mou, J.-Y., Lyu, J.-W., Di, Y.-W., Liao, Y.-L., & Wang, L. (2023). Rapid discrimination of Shigella spp. and Escherichia coli via label-free surface enhanced Raman spectroscopy coupled with machine learning algorithms. *Frontiers in Microbiology, 14*.

Ma, P., Liang, F., Sun, Y., Jin, Y., Chen, Y., Wang, X., & Song, D. (2013). Rapid determination of melamine in milk and milk powder by surface-enhanced Raman spectroscopy and using cyclodextrin-decorated silver nanoparticles. *Microchimica Acta, 180*, 1173–1180.

Matsuda, S. (1984). Transfer of antibiotics into maternal milk. *Biological Research in Pregnancy and Perinatology, 5*(2), 57–60.

Miao, H., Wang, Y., & Yang, X. (2018). Carbon dots derived from tobacco for visually distinguishing and detecting three kinds of tetracyclines. *Nanoscale, 10*(17), 8139–8145.

Mileva, R. (2019). Determination of free doxycycline concentrations in the plasma and milk of sheep and in the plasma of rabbits by using the HPLC method. *Macedonian Veterinary Review, 42*(2), 123–130.

Mu, G., Liu, H., Xu, L., Tian, L., & Luan, F. (2012). Matrix solid-phase dispersion extraction and capillary electrophoresis determination of tetracycline residues in milk. *Food Analytical Methods, 5*, 148–153.

Mueller, I., & Tronick, E. (2019). Early life exposure to violence: Developmental consequences on brain and behavior. *Frontiers in Behavioral Neuroscience, 13*, 156.

Niebyl, J. R. (2003). Antibiotics and other anti-infective agents in pregnancy and lactation. *American Journal of Perinatology, 20*(08), 405–414.

Organization, W. H. (2010). *Strontium and strontium compounds. In strontium and strontium compounds (pp. iv, 63-iv, 63)*.

Perales-Rondon, J. V., Colina, A., Gonzalez, M. C., & Escarpa, A. (2020). Roughened silver microtubes for reproducible and quantitative SERS using a template-assisted electrosynthesis approach. *Applied Materials Today, 20*, Article 100710.

Pinheiro, P. C., Fateixa, S., Nogueira, H. I., & Trindade, T. (2018). Magnetite-supported gold nanostars for the uptake and SERS detection of tetracycline. *Nanomaterials, 9*(1), 31.

Prado, C. K., Ferreira, F. D., Bando, E., & Machinski, M., Jr. (2015). Oxytetracycline, tetracycline, chlortetracycline and doxycycline in pasteurised cow's milk commercialised in Brazil. *Food Additives & Contaminants: Part B, 8*(2), 81–84.

Ramezani, M., Danesh, N. M., Lavaee, P., Abnous, K., & Taghdisi, S. M. (2015). A novel colorimetric triple-helix molecular switch aptasensor for ultrasensitive detection of tetracycline. *Biosensors and Bioelectronics, 70*, 181–187.

Sagar, D., Kuanglin, C., Huang, Q., Kim, M., & Schmidt, W. (2018). J. Qin and CL Broadhurst,"Simple surface-enhanced Raman spectroscopic method for on-site screening of tetracycline residue in whole milk,". *Sensors, 18*, 424.

Sivakesava, S., & Irudayaraj, J. (2002). Rapid determination of tetracycline in milk by FT-MIR and FT-NIR spectroscopy. *Journal of Dairy Science, 85*(3), 487–493.

Tackman, E. C., Trujillo, M. J., Lockwood, T.-L. E., Merga, G., Lieberman, M., & Camden, J. P. (2018). Identification of substandard and falsified antimalarial pharmaceuticals chloroquine, doxycycline, and primaquine using surface-enhanced Raman scattering. *Analytical Methods, 10*(38), 4718–4722.

Thrift, W. J., Ronaghi, S., Samad, M., Wei, H., Nguyen, D. G., Cabuslay, A. S., & Hochbaum, A. I. (2020). Deep learning analysis of vibrational spectra of bacterial lysate for rapid antimicrobial susceptibility testing. *ACS Nano, 14*(11), 15336–15348.

Toma, K., Oishi, K., Iitani, K., Arakawa, T., & Mitsubayashi, K. (2022). Surface plasmon-enhanced fluorescence immunosensor for monitoring cardiac troponin I. *Sensors and Actuators B: Chemical, 368*, Article 132132.

Usman, M., Guo, X., Wu, Q., Barman, J., Su, S., Huang, B., & Zhan, Q. (2019). Facile silicone oil-coated hydrophobic surface for surface enhanced Raman spectroscopy of antibiotics. *RSC Advances, 9*(25), 14109–14115.

Usman, M., Ishafaq, M., Muhammad, Z., Ali, W., Dastgeer, G., Zhang, X., & Wang, L. (2023). Evaporation-induced self-assembly of gold nanorods on a hydrophobic substrate for surface enhanced Raman spectroscopy applications. *Frontiers in Materials, 9*, 1048011.

Usman, M., Tang, J.-W., Li, F., Lai, J.-X., Liu, Q.-H., Liu, W., & Wang, L. (2022). Recent advances in surface enhanced Raman spectroscopy for bacterial pathogen identifications. *Journal of Advanced Research, 51*, 91–107.

Usman, M., Tang, J.-W., Li, Z.-K., Lai, J.-X., Yuan, K.-X., Liu, Q.-H., & Wang, L. (2023). Historical review of SERS in biomedical applications: Infectious diseases. In *SERS-based advanced diagnostics for infectious diseases*. Bristol, UK: IOP Publishing (pp. 3-1-3-34).

Wang, L., Tang, J.-W., Li, F., Usman, M., Wu, C.-Y., Liu, Q.-H., & Gu, B. (2022). Identification of bacterial pathogens at genus and species levels through combination of Raman spectrometry and deep-learning algorithms. *Microbiology Spectrum, 10*(6). e02580–02522.

Wang, L., Zhang, X.-D., Tang, J.-W., Ma, Z.-W., Usman, M., Liu, Q.-H., & Gu, B. (2022). Machine learning analysis of SERS fingerprinting for the rapid determination of mycobacterium tuberculosis infection and drug resistance. *Computational and Structural Biotechnology Journal, 20*, 5364–5377.

Wang, T., Liu, M., Huang, S., Yuan, H., Zhao, J., & Chen, J. (2021). Surface-enhanced Raman spectroscopy method for classification of doxycycline hydrochloride and tylosin in duck meat using gold nanoparticles. *Poultry Science, 100*(6), Article 101165.

Wei, S., Du, W., Hao, Z., Li, N., Li, Y., & Wang, M. (2024). Construction of dense film inside capillary wall and SERS application research. *Spectrochimica Acta Part A: Molecular and Biomolecular Spectroscopy, 310*, Article 123967.

Xie, Y., Zhu, X., Sun, Y., Wang, H., Qian, H., & Yao, W. (2012). Rapid detection method for nitrofuran antibiotic residues by surface-enhanced Raman spectroscopy. *European Food Research and Technology, 235*, 555–561.

Xu, H., Mi, H.-Y., Guan, M.-M., Shan, H.-Y., Fei, Q., Huan, Y.-F., & Feng, G.-D. (2017). Residue analysis of tetracyclines in milk by HPLC coupled with hollow fiber membranes-based dynamic liquid-liquid micro-extraction. *Food Chemistry, 232*, 198–202.

Xu, R., Shen, Z., Xiang, Y., Huang, J., Wang, G., Yang, F., & Duan, X. (2023). Portable electrochemiluminescence detection system based on silicon photomultiplier single photon detector and aptasensor for the detection of tetracycline in milk. *Biosensors and Bioelectronics, 220*, Article 114785.

Xu, Z., Wang, Z., Liu, M., Yan, B., Ren, X., & Gao, Z. (2020). Machine learning assisted dual-channel carbon quantum dots-based fluorescence sensor array for detection of tetracyclines. *Spectrochimica Acta Part A: Molecular and Biomolecular Spectroscopy, 232*, Article 118147.

Yang, J. L., Yang, Z. W., Zhang, Y. J., Ren, H., Zhang, H., Xu, Q. C., & Tian, Z. Q. (2017). Quantitative detection using two-dimension shell-isolated nanoparticle film. *Journal of Raman Spectroscopy, 48*(7), 919–924.

Yang, L., & Shami, A. (2020). On hyperparameter optimization of machine learning algorithms: Theory and practice. *Neurocomputing, 415*, 295–316.

Yang, Z., Ma, C., Gu, J., Wu, Y., Zhu, C., Li, L., & Wang, C. (2021). A sensitive surface-enhanced Raman spectroscopy method for detecting tetracycline in milk. *Applied Spectroscopy, 75*(5), 589–595.

Yu, L., Chen, H., Yue, J., Chen, X., Sun, M., Hou, J., & Wang, S. (2020). Europium metal-organic framework for selective and sensitive detection of doxycycline based on fluorescence enhancement. *Talanta, 207*, Article 120297.

Yuan, W., Han, X., Shi, G., Wang, M., Zhou, W., Cui, J., & Wang, L. (2024). Machine learning-driven multi-level composite SERS platform for trace detection of chlorogenic acid as pharmacodynamic substance in honeysuckle. *Optics & Laser Technology, 169*, Article 109911.